Competitive Inner-Imaging Squeeze and Excitation for Residual Network

Yang Hu, Guihua Wen*, Mingnan Luo†, Dan Dai, Jiajiong Ma

School of Computer Science & Engineering, South China University of Technology {cssuperhy@mail., crghwen@, csluomingnan@mail., csdaidan@mail., csmajiajiong@mail.}scut.edu.cn

Abstract

Residual Networks make the very deep convolutional architecture works well, which use the residual unit to supplement the identity mappings. On the other hand, Squeeze-Excitation (SE) network propose an adaptively recalibrates channel-wise attention approach to model the relationship of feature maps from different convolutional channel. In this work, we propose the competitive SE mechanism for residual network, rescaling value for each channel in this structure will be determined by residual and identity mappings jointly, this design enables us to expand the meaning of channel relationship modeling in residual blocks: the modeling of competition between residual and identity mappings make identity flow can controll the complement of residual feature maps for itself. Further, we design a novel pair-view competitive SE block to shrink the consumption and re-image the global characterizations of intermediate convolutional channels. We carry out experiments on datasets: CIFAR, SVHN, ImageNet, the proposed method can be compared with the state-of-the-art results.

Introduction

Deep convolution neural networks (CNNs) have shown great effectiveness to tackling and modeling image data (Krizhevsky, Sutskever, and Hinton 2012; Szegedy et al. 2015; Szegedy et al. 2016; Simonyan and Zisserman 2015). The presentation of Residual Network (ResNet) enables the network structure go very deeper and achieve better performance (He et al. 2016a). At the same time, attention has also been paid to the modeling of implicit relationships in CNNs (Chen et al. 2017a; Wang et al. 2017a), and the "Squeeze-Excitation" (SE-Net) architecture (Hu, Shen, and Sun 2018) capture the channel relationship with cheap cost which can be used directly in all kinds of CNNs. However, when SE-block is applied in ResNet, the identity mapping has not been taken into the input of channel-wise attention of residual flow. As analysis of ResNet, the residual mapping can be regarded as a supplement to identical mapping (He et al. 2016b), and with the increase of depth, residual network shows some redundancy (Huang et al. 2016; Veit, Wilber, and Belongie 2016), thus, identity mappings should also be taken into consideration of channel attention, and make the supplement for itself more dynamic and precise. In this work, we design a new competitive squeeze and excitation architecture based on SE-block, named Competitive SE (CMPE-SE) network. We plan to expand the factors which considered in channel re-weight of residual mappings and use the CMPE-SE design to model the implicit competitive relationship between identity and residual feature maps. Furthermore, we try different modes of feature maps merging and used convolution to capture channel-wise features.

Compare with the typical SE building block, the composition of CMPE-SE block is illustrated as Fig. 1. The basic mode of CMPE-SE module absorb the compressed signals for identity mappings $X \in \mathbb{R}^{W' \times H' \times C'}$ and residual mappings $U \in \mathbb{R}^{W \times H \times C}$ meanwhile with the same squeeze operation in reference (Hu, Shen, and Sun 2018), concatenate and embed them jointly and multiply the excitation value back to each channel; A evolutionary version of CMPE-SE block is designed to merge the global distributions from residual and identity feature maps in the way of above and below stacking, then uses convolution with size 2×1 or 1×1 to gain the paired or interlaced relations of channels from different sides.

As the design of CMPE-SE module considers residual and identity flow joinly based on the original SE block for ResNet, it expand the task and meaning of "Squeeze and Excitation" which recalibrate the channel-wise features, the modeling object of CMPE-SE unit is not limited to the relationship of the residual channels, but the relationship between all residual and identity feature maps, as well as the competition between residual and identity flows. In this way, the network can dynamically adjust the complement weights of residual channels to the identity mapping by using the competitive relations in each residual block. Further, stacking of the squeezed channel features and convolution scanning can be seen as a kind of re-imaging for network internal representation.

The exploration of convolution network architecture and the modeling of network internal representation is a meaningful and challenging task (Xie and Yuille 2017; Zoph et al. 2018; Real et al. 2018), usually with high complicacy (Zhang et al. 2017b; Wang et al. 2018). By comparison, the layout of CMPE-SE module outlined above is easy to implement and can be cheaply applied to the residual network and its all variants. The contributions of this study can be listed as follows:

1. We propose a new competitive "Squeeze and Excitation"

^{*}corresponding author

[†]equally contribution with Guihua Wen

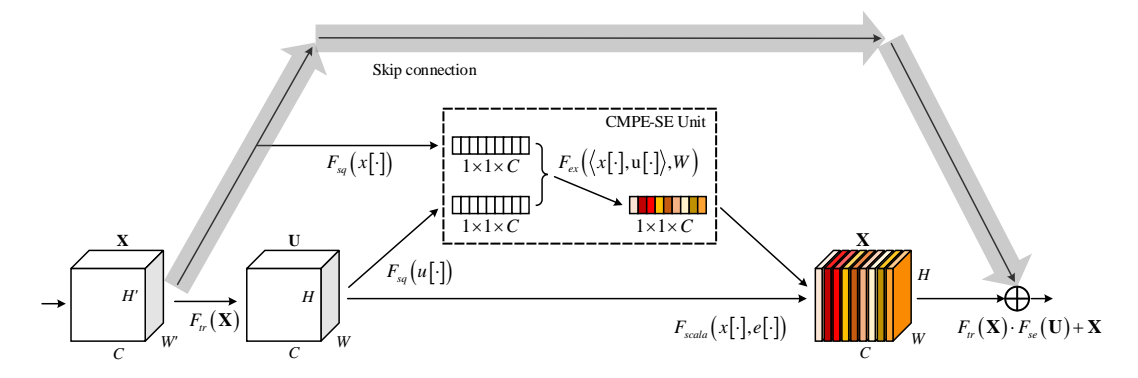


Figure 1: Competitive Squeeze-Excitation Architecture for Residual block.

unit for residual network, which jointly model the relationship of residual and identity channels, so the identity mapping can join in the re-weighting for residual channels.

- 2. We present a design of re-imaging for intermediate structure representation in CNNs, thus to re-scan the channel relation features with convolutional filters.
- 3. We conduct experiments on several datasets including CIFAR-10, CIFAR-100, SVHN and ImageNet to validate the performance of the presented models.

Related Work

Residual architectures. ResNet (He et al. 2016a) has become popular in virtue of its assistance in deep model training. Many works based on it improve performance by expanding its structure (Zagoruyko and Komodakis 2016; Han, Kim, and Kim 2017; Xie et al. 2017; Zhang et al. 2017b) or uses its explanation of ordinary differential equations to explore its reversible form (Chang et al. 2018; Chen et al. 2018). Because ResNet is internal diverse without the operation like "drop-path" (Larsson, Maire, and Shakhnarovich 2017) and is proved to be structurally redundant (Veit, Wilber, and Belongie 2016), destructive approaches can promote its efficiency and enrich the structure representation by means of policy learning (Wu et al. 2018; Wang et al. 2017b) or dynamic exit strategy (Figurnov et al. 2017; Huang et al. 2017a).

An parallel line of research deem that the intermediate feature maps should be modeled repeatedly (Huang et al. 2017b). This compact architecture enables intermediate features to be refined and expanded, thereby enhance the representation ability with concentrated parameter size. (Yang et al. 2018) proposes a more compact model by circulating the densely block. Further, dual path networks (DPN) (Chen et al. 2017b) combines the advantages of ResNet and DenseNet, and make the residual units to extra model the relationship between identity flow and densely connected flow. A trend of compact architectures is to expand the mission of network subassemblies while refining the intermediate features. Based on SE block (Hu, Shen, and Sun 2018), our proposed CMPE-SE design also refines the intermediate features and develops the job of the SE unit, the difference is that our model focuses on self-controlling of components in ResNet, rather than simply feature reusing. Moreover, re-imaging of channel signals presents a novel modeling view of intermediate features.

Attention and gating mechanisms in CNNs. Attention is widely applied in the modeling process of CNNs (Nguyen, Zhao, and Yan 2018) and typically used to re-weight the image spatial signals (Wang et al. 2017a; Li, Zhu, and Gong 2018; Zheng et al. 2017; Sun et al. 2018), including multiscale (Chen et al. 2016; Newell, Yang, and Deng 2016) and multi-shape (Jaderberg et al. 2015) features. As a tool to bias the allocation of resources (Hu, Shen, and Sun 2018), attention is also used to regulate the internal features of CNNs (Perez et al. 2018; Stollenga et al. 2014). Unlike channel switching, combination (Zhang et al. 2017a; Zhang et al. 2018b) or using reinforcement learning to reorganize the network paths (Ahmed and Torresani 2017), channel-wise attention, typical such as (Hu, Shen, and Sun 2018), provides a end to end training solution to re-weight the intermediate channel features, at the same time, some models combine spatial attention and channel-wise attention (Chen et al. 2017a; Linsley et al. 2018), and their modeling scope is still limited in total attentional elements. In contrast, our proposed CMPE-SE block considers the extra related factors (identity mappings) besides the objects of attention (residual mappings), additionally, we test the effect of filters in channel-wise attention with channel signal re-imaging.

Competitive Squeeze Excitation Blocks

Residual block is routinely defined as the amalgamation of identity mapping $\mathbf{X} \in \mathbb{R}^{W' \times H' \times C'}$ and residual mapping $\mathbf{U} \in \mathbb{R}^{W \times H \times C}$, as follows:

$$y = F_{res}(\mathbf{x}, \mathbf{w}_r) + \mathbf{x}. \tag{1}$$

We record the output of residual mapping as $U_r = F_{res}(x, w_r) = [u_r^1, u_r^2, \dots, u_r^C]$. As described in the design of SE-Net, the "Squeeze-Excitation" module (Hu, Shen, and Sun 2018) control the re-weighted value of convolution feature maps including residual mappings, as follows:

$$\hat{u}_r^c = F_{sq}(\mathbf{u}_r^c) = \frac{1}{W \times H} \sum_{i=1}^W \sum_{j=1}^H u_r^c(i,j), \qquad (2)$$

$$s = F_{ex}(\hat{u}_r, w_{ex}) = \sigma(ReLU(\hat{u}_r, w_1), w_2),$$
 (3)

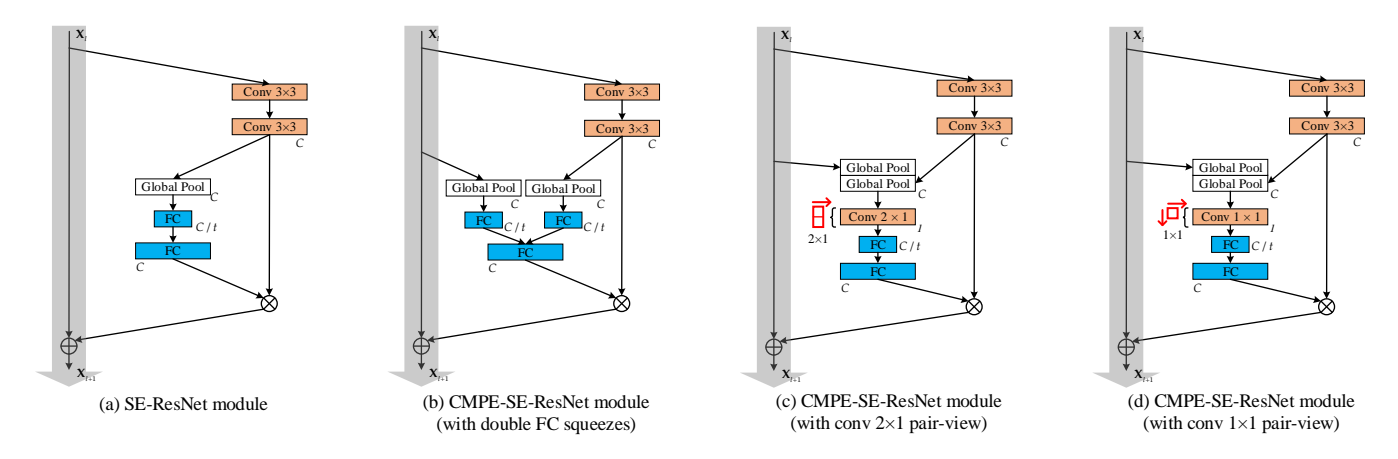


Figure 2: Difference of SE-ResNet module and CMPE-SE-ResNet modules. (a) Typical SE Residual block, the orange rectangles represent the convolution and blue indicates fully connected layer, the white one is global average pooling. (b) CMPE-SE residual block of the version with double fully connected embedding for squeezed signals, which are merged in the excitation layer. (c) CMPE-SE residual block with 2×1 convolutional pair-view, after stacking the squeezed signals, the red pane and arrow indicate the size and the scanning direction of concolution. (d) CMPE-SE residual block with 1×1 convolutional pair-view.

$$\tilde{\mathbf{x}}_c = F_{scale}(\mathbf{s}_c, \mathbf{u}_r^c)
= F_{se}(\mathbf{u}_r)[\cdot] \times F_{res}(\mathbf{x}, \mathbf{w}_r)[\cdot] = \mathbf{s}_c \cdot \mathbf{u}_r^c,$$
(4)

where \hat{u}^c_r refers to the global pooling result of squeeze operation and $\sigma(\cdot)$ denotes the sigmoid activation, operators \times and \cdot are element-wise multiplication. The excitation contains two fully-connected (FC) layers, the weights $w_1 \in \mathbb{R}^{\frac{C}{t} \times C}$ means dimensionality-reduction with ratio t (set to 16 by default) and $w_2 \in \mathbb{R}^{C \times \frac{C}{t}}$, so the variable s is the rescaling tensor for residual channels. We can summarize the flow of residual block in SE-ResNet as:

$$y = F_{se}(\mathbf{u}_r) \cdot F_{res}(\mathbf{x}, \mathbf{w}_r) + \mathbf{x}. \tag{5}$$

Stated thus, conventional SE operation models the relationship of convolution channels and feedback with recalibrate values which are calculated only with the feature maps of residual flow in ResNet.

Competition between Residual and Identity Flows

The architecture of the current SE-ResNet shows that the rebuilding weights are not the products of the joint decision with identity and residual mappings. From an intuitional point of view, we introduce the identity flow into the process of "Squeeze-Excitation".

Corresponding to the residual mapping U_r , the global information embedding from identity mapping $X_{id} = [x_{id}^1, x_{id}^2, \dots, x_{id}^C]$ can also be gained as:

$$\hat{x}_{id}^c = F_{sq}(\mathbf{x}_{id}^c) = \frac{1}{W \times H} \sum_{i=1}^W \sum_{j=1}^H x_{id}^c(i,j), \quad (6)$$

same as \hat{u}_r^c , \hat{x}_{id}^c is the global average pooling of identity features, and it is used as a part of joint input for residual channels recalibration, together with \hat{u}_c^c :

$$\mathbf{s} = F_{ex}(\hat{\mathbf{u}}_r, \hat{\mathbf{x}}_{id}, \mathbf{w}_{ex})$$

$$= \sigma \left(\langle ReLU(\hat{\mathbf{u}}_r, \mathbf{w}_1^r), ReLU(\hat{\mathbf{x}}_{id}, \mathbf{w}_1^{id}) \rangle, \mathbf{w}_2^{ex} \right), \tag{7}$$

$$\tilde{\mathbf{x}}_c = F_{se}(\mathbf{u}_r, \mathbf{x}_{id})[\cdot] \times F_{res}(\mathbf{x}_{id}, \mathbf{w}_r)[\cdot] = s_c \cdot \mathbf{u}_r^c, \quad (8)$$

where parameters $\mathbf{w}_1^r \in \mathbb{R}^{\frac{C}{t} \times C}$ and $\mathbf{w}_1^{id} \in \mathbb{R}^{\frac{C}{t} \times C}$ encode the squeezed signals from identity and residual mappings and followed by another FC layer parameted by $\mathbf{w}_2^{ex} \in \mathbb{R}^{C \times \frac{2C}{t}}$ with C neurones.

The competition between residual and identity mappings is modeled by the CMPE-SE module introduced above and react to each residual channels. Implicitly, we can think that the winning of the identity channels in this competition brings less weights of the residual channels, on the other hand, the weights of the residual channels will increase. Finally, the CMPE-SE residual block is reformulated as:

$$y = F_{se}(\mathbf{u}_r, \mathbf{x}_{id}) \cdot F_{res}(\mathbf{x}_{id}, \mathbf{w}_r) + \mathbf{x}_{id}. \tag{9}$$

Fig. 2(a) and (b) show the difference between the typical SE and the CMPE-SE residual modules. The embedding of squeezed signals $\hat{\mathbf{u}}_r = [\hat{u}_r^1, \hat{u}_r^2, \dots, \hat{u}_r^C]^{\top}$ and $\hat{\mathbf{x}}_{id} = [\hat{x}_{id}^1, \hat{x}_{id}^2, \dots, \hat{x}_{id}^C]^{\top}$ are simply concatenated before excitation. Here, the back-propagation algorithm optimizes two intertwined parts of modeling processes: (1) relationship of all channel in residual block; (2) competition between residual and identity channels. In addition, \mathbf{w}_1^{id} is the only extra parameter cost.

Pair-View Re-imaging for Intermediate Channel Features

In basic mode of CMPE-SE residual block, one additional fully connected encoder is needed to joint modeling the competition of residual and identity channels. We also design the pair-view strategies of competitive "Squeeze-Excitation", to save parameters and capture the channel relation features from a novel angle. Fig. 2(c) and (d) show their structure.

Firstly, stacked squeezed feature maps are generated as:

$$\hat{\mathbf{v}}_s = \begin{bmatrix} \hat{\mathbf{u}}_r^\top \\ \hat{\mathbf{x}}_{id}^\top \end{bmatrix} = \begin{bmatrix} \hat{u}_r^1, & \hat{u}_r^2 & \cdots & \hat{u}_r^C \\ \hat{x}_{id}^1, & \hat{x}_{id}^2 & \cdots & \hat{x}_{id}^C \end{bmatrix}, \tag{10}$$

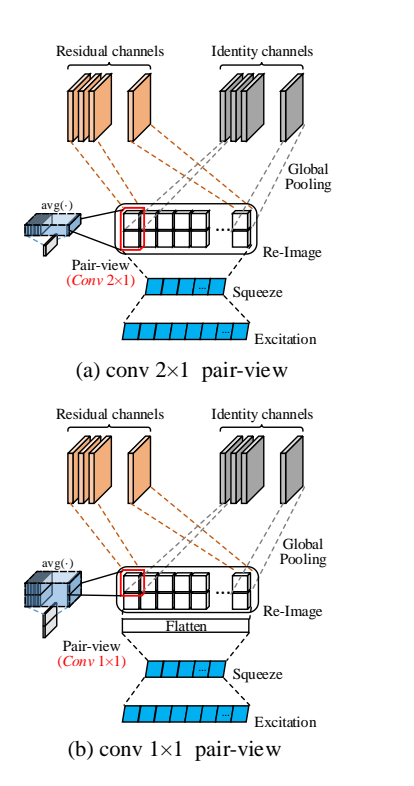


Figure 3: Pair-view modes of Competitive Squeeze and Excitation with convolution 2×1 and 1×1 .

the pair-view re-imaging acquire feature maps of channel relation rather than original picture input. we use ε filters $\{\mathbf w^1_{(2\times 1)},\dots,\mathbf w^\varepsilon_{(2\times 1)}\}$, $\mathbf w^i_{(2\times 1)}=[w^i_{11},w^i_{21}]^{\top}$ scan the stacked tensor of squeezed features from residual and identity channels, then average the pair-view output,

$$\mathbf{v}_c = \frac{1}{\epsilon} \sum_{i=1}^{\epsilon} \left(\hat{\mathbf{v}}_s * \mathbf{w}_{(2 \times 1)}^i \right)^\top, \tag{11}$$

here * denotes convolution and v_c is the re-imaged feature map, batch normalization (BN) (Ioffe and Szegedy 2015) is performed right after convolution. Next, there are re-imaged signal encoding and excitation, as follows:

$$s = \sigma \left(\mathbf{w}_2^{ex} \cdot ReLU(\mathbf{w}_1 \cdot \mathbf{v}_c) \right), \tag{12}$$

where squeeze encoder is parameted by $\mathbf{w}_1 \in \mathbb{R}^{\frac{C}{t} \times C}$ now and excitation parameters are also shrunk to $\mathbf{w}_2^{ex} \in \mathbb{R}^{C \times \frac{C}{t}}$. Fig. 3(a) shows the detailed structure of "Conv (2×1) " pair-view CMPE-SE unit.

The "Conv (2×1) " pair-view strategy models the competition between residual and identity channels based on strict upper and lower positions, which ignores a factor that any feature signal in re-imaged tensor could be associated with any other signal not only in the location of vertical direction. Based on this consideration, we use a 1×1 convolution kernel $\mathbf{w}^i_{(1 \times 1)} = [w^i_{11}]$ to replace above $\mathbf{w}^i_{(2 \times 1)} = [w^i_{11}, w^i_{21}]^\top$, furthermore, a flatten layer is used to reshape the output of 1×1 convolution:

$$\mathbf{v}_c' = \frac{1}{\varepsilon} \sum_{i=1}^{\varepsilon} \left(\hat{\mathbf{v}}_s * \mathbf{w}_{(1 \times 1)}^i \right), \tag{13}$$

$$s = \sigma\left(w_2^{ex} \cdot ReLU\left(w_1 \cdot \left(F_{flatten}\left(v_c'\right)\right)^{\top}\right)\right), \quad (14)$$

where $\mathbf{v}_c = (F_{flatten} \ (\mathbf{v}_c'))^{\top}$ corresponds to Eq. 11, and the parameter size of the encoder will return to $\mathbf{w}_1 \in \mathbb{R}^{\frac{C}{t} \times 2C}$, excitation is still $\mathbf{w}_2^{ex} \in \mathbb{R}^{C \times \frac{C}{t}}$. Fig. 3(b) depicts the "Conv (1×1) " pair-view CMPE-SE unit. In fact, this mode can be regarded as a simple linear transformation for combined squeezed signals before embedding. The number of pair-view convolution kernels ε above-mentioned is set as: the block width divided by the dimensionality-reduction ratio t.

Experiments

We evaluate our approach on datasets CIFAR-10, CIFAR-100, SVHN and ImageNet. We train several basic ResNets and compare the performances with/without CMPE-SE module. Then, we challenge the state-of-the-art results.

Datasets and Settings

CIFAR. The CIFAR-10 and CIFAR-100 datasets are 32×32 colored images (Krizhevsky 2009). They both contains 60,000 images belonging to 10 and 100 classes, and 50,000 images for training, 10,000 images for testing. We subtract the mean and divide by the standard deviation for data normalization, and the standard data augmentation (translation/mirroring) is adopted for the training sets.

SVHN. The Street View House Number (SVHN) datasets (Netzer et al. 2011) contains 32×32 colored images of 73,257 samples in training set and 26,032 for testing and 531,131 digits for additional training. We divide images by 255 and use all training data without data augmentation.

ImageNet. ILSVRC 2012 dataset (Deng et al. 2009) contains 1.2 million training images, 50,000 validation images and 100,000 for testing with 1,000 classes. standard data augmentation is adopted for training set and the 224×224 crop is randomly sampled. All images are normalized into [0,1] with mean values and standard deviations.

Settings. We firstly test the effectiveness of CMPE-SE modules on two classical models: pre-act ResNet (He et al. 2016b) and Wide Residual Network (Zagoruvko and Komodakis 2016) with CIFAR-10 and CIFAR-100, we also re-implement the typical SE block (Hu, Shen, and Sun 2018) based on them. For fair comparison, we follow basic structures and hyper-parameters turning in the original papers, more implementation details is available at the open source¹. We train our models by optimizer stochastic gradient descent (SGD) with 0.9 Nesterov momentum, and use batch size 128 for 200 epochs, the learning rate is initialized to 0.1 and divided by 10 at 100th, 150th epochs for pre-act ResNet, divided by 5 at epochs 60, 120, 160 for WRN. Secondly, we increase the number of training epochs to 300 (divide learning rate at epochs 120, 200, 260) to challenge the state-of-the-art results. The *mixup* is a advanced training strategy on convex combinations of sample pairs and their labels (Zhang et al.

¹https://github.com/scut-aitcm/CompetitiveSENet

Model (# parames)	C10	C10 mixup
ResNet-110 (1.7M)	6.37	_
ResNet-164 (1.7M)	5.46	4.15
SE-ResNet-110 (1.75M)	5.68	_
SE-ResNet-164 (1.95M)	4.85	4.07
CMPE-SE-ResNet-110 (Ours)		
-1×1 pair-view (1.76M)	5.45	4.30
CMPE-SE-ResNet-164 (Ours)		
- double FC (2.12M)	4.72	3.82
-2×1 pair-view (1.95M)	4.59	3.76
-1×1 pair-view (2.04M)	4.57	3.78
	C100	C100 mixup
ResNet-110 (1.7M)	_	23.98
ResNet-164 (1.7M)	24.33	20.84
SE-ResNet-110 (1.75M)	25.82	_
SE-ResNet-164 (1.95M)	22.61	19.89
CMPE-SE-ResNet-110 (Ours)		
-1×1 pair-view (1.76M)	25.35	22.92
CMPE-SE-ResNet-164 (Ours)		
- double FC (2.12M)	22.38	19.58
-2×1 pair-view (1.95M)	22.41	19.69
-1×1 pair-view (2.04M)	22.35	19.46

Table 1: Error rates(%) of pre-act ResNets on datasets CIFAR-10 and CIFAR-100.

2018a), we apply it to the aforementioned evaluations and add 20 epochs with traditional strategy after formal training process of *mixup*. On SVHN, our models are trained for 160 epochs, the initial learning rate is 0.01 and is divided by 10 at 80th and 120th epochs. On ImageNet, we train models for 100 epochs with a batch size 64, the initial learning rate is 0.1 and is reduced by 10 times at epoch 30, 60 and 90.

Results on CIFAR and SVHN

The results of contrast experiments for ResNets with/without CMPE-SE module are shown in Table. 1 and 2, and we use pre-act ResNet (He et al. 2016b) by default, the numbers of parameters are recorded in brackets and the best records are marked by bold. By analysing these results, we can draw the following conclusions:

CMPE-SE block can achieve superior performance than SE block both on the classical ResNets and the wide ResNets, it drops error rate of SE-ResNet by 0.226% averagely and 0.312% for WRN, and does not consume too much extra parameters($0.2\%\sim5\%$ than SE Residual Network). The pair-view mode of CMPE-SE units with 1×1 convolution can get better results than the basic mode, and use less parameters, which means hybrid modeling of squeezed signals is more effective than merge them after embedding. Another phenomenon is that CMPE-SE module can drop the error rate more efficaciously on WRN model than on traditional ResNet, therefore, the fewer number of layers and the wider residual in "dumpy" wide ResNet can better reflect the role of identity mapping in residual channel-wise attention.

By observing the performance of ResNets under different

Model (# parames)	C10	C10 mixup
WRN-22-10 (26.8M)	4.44	_
WRN-28-10 (36.5M)	4.17	2.70
SE-WRN-22-10 (27.0M)	4.09	_
SE-WRN-28-10 (36.8M)	3.88	2.68
CMPE-SE-WRN-16-8 (Ours)		
-1×1 pair-view (11.1M)	4.20	3.18
CMPE-SE-WRN-22-10 (Ours)		
-1×1 pair-view (27.1M)	3.75	2.86
CMPE-SE-WRN-28-10 (Ours)		
– <i>double FC</i> (37.0M)	3.66	2.62
-2×1 pair-view (36.8M)	3.73	2.65
-1×1 pair-view (36.9M)	3.58	2.58
	C100	C100 mixup
WRN-22-10 (26.8M)	20.75	17.88
WRN-28-10 (36.5M)	20.50	17.50
SE-WRN-22-10 (27.0M)	19.52	17.06
		17.00
SE-WRN-28-10 (36.8M)	19.05	16.77
SE-WRN-28-10 (36.8M) CMPE-SE-WRN-16-8 (Ours)	19.05	
	19.05 19.77	
CMPE-SE-WRN-16-8 (Ours)		16.77
CMPE-SE-WRN-16-8 (Ours) - 1 × 1 pair-view (11.1M)		16.77
CMPE-SE-WRN-16-8 (Ours) - 1 × 1 pair-view (11.1M) CMPE-SE-WRN-22-10 (Ours)	19.77	16.77
CMPE-SE-WRN-16-8 (Ours) - 1 × 1 pair-view (11.1M) CMPE-SE-WRN-22-10 (Ours) - 1 × 1 pair-view (27.1M)	19.77	16.77
CMPE-SE-WRN-16-8 (Ours) - 1 × 1 pair-view (11.1M) CMPE-SE-WRN-22-10 (Ours) - 1 × 1 pair-view (27.1M) CMPE-SE-WRN-28-10 (Ours)	19.77 18.86	16.77 17.26 16.82

Table 2: Error rates(%) of Wide Residual Networks on datasets CIFAR-10 and CIFAR-100.

scales, CMPE-SE unit enables smaller networks to achieve or even exceed the same structure with more parameters. For WRN, the classification results of CMPE-SE-WRN-16-8 are same with or go beyond of WRN-28-10, and the results of CMPE-SE-WRN-22-10 is better than of SE-WRN-28-10.

The *mixup* (Zhang et al. 2018a) can be seen as an advanced approach of data augmentation, which can improve the generalization ability of models. In the case of used the *mixup*, CMPE-SE block can further improve the performance of the residual networks until achieve the state-of-the-art results.

Fig.4 shows training curves on different modes of preact ResNet-164 and WRN-28-10, which include: basic SE Residual Networks and CMPE-SE residual networks with double FC encoding and 1×1 pair-view re-imaging. In these curves, we can find out: the decline of the training loss of the CMPE-SE residual networks is slightly better than of the typical SE ResNets.

Table. 3 lists the challenge results of CMPE-SE-WRN-28-10 and CMPE-SE-WRN-40-10 with state-of-the-art results, we train the above two models for 300 epochs. The compared networks include: original ResNet (He et al. 2016a), pre-act ResNet (He et al. 2016b), ResNet with Stochastic Depth (Huang et al. 2016), FractalNet (Larsson, Maire, and Shakhnarovich 2017), DenseNet (Huang et al. 2017b), ResNeXt (Xie et al. 2017), PyramidNet (Han, Kim, and Kim 2017) and CliqueNet (Yang et al. 2018), We can notice that our models based on wide residual networks can get compara-

Model	depth	# parames	C10	C10 mixup	C100	C100 mixup	SVHN
original ResNet	110	1.7M	6.43	_	25.16	_	_
pre-act ResNet-18	18	11.7M	_	4.20	_	21.10	_
Stochastic Depth	110	1.7M	5.23	_	24.58	_	1.75
FractalNet	21	38.6M	4.60	_	23.73	_	1.87
DenseNet	100	27.2M	3.74	_	19.25	_	1.59
DenseNet-BC	190	25.6M	3.46	2.70	17.18	16.80	_
ResNeXt-29	29	34.4M	3.65	_	17.77	_	_
PyramidNet (α = 270)	110	28.3M	3.73	_	18.25	_	_
– bottleneck	164	27.0M	3.48	_	17.01	_	_
CliqueNet-30	30	10.02M	5.06	_	21.83	_	1.64
CMPE-SE-WRN-28-10 (Ours)							
– double FC	28	37.04M	3.60	2.60	18.49	15.90	1.61
-1×1 pair-view	28	36.92M	3.55	2.54	18.42	15.94	1.59
CMPE-SE-WRN-40-10 (Ours)							
-1×1 pair-view	40	56.50M	3.52	2.45	18.54	15.62	_

Table 3: Error rates(%) of different methods on datasets CIFAR-10, CIFAR-100 and SVHN, the best records of our models are **bold** and the best results are highlighted in **red**.

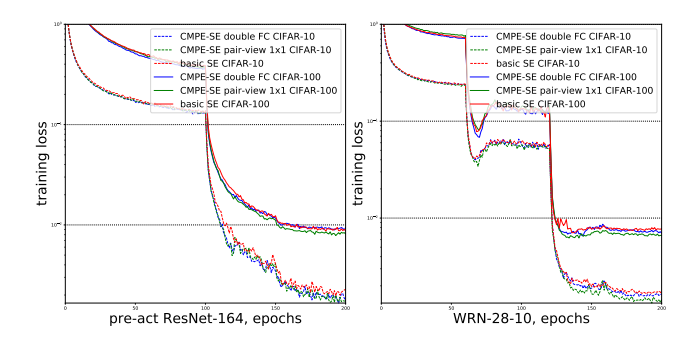


Figure 4: Training curves of basic SE residual network and different modes of CMPE-SE residual network, on CIFAR-10 and CIFAR-100. Left: different version of SE pre-act ResNet-164 for 200 epochs. Right: different version of SE WRN-28-10 for 200 epochs.

ble or better performance than compared models. Moreover, we know that although the parameter size it takes is large, the training speed of WRN is much faster than DenseNets, even faster than ResNets (Zagoruyko and Komodakis 2016).

After 300 epochs of training for models CMPE-SE-WRN-28-10 and CMPE-SE-WRN-40-10, we discover that the result of the 200 epochs of training is not much worse than that of the 300 epochs, so we can infer that the CMPE-SE residual networks are not hungry for a lot of training.

Results on ImageNet

Due to the limitation of computational resource (GTX 1080Ti \times 2), we only test the performance of pre-act ResNet-50 (ImageNet mode) after equipped with CMPE-SE blocks, and we use the smaller mini-batch with size of 64, instead of 256 in most studies.

Although a smaller batch-size would impair the performance training for the same epochs (Yang et al. 2018), the results of CMPE-SE-ResNet-50 (both double FC and 1×1

Model	top-1	top-5
ResNet-18	30.43	10.76
ResNet-34	26.73	8.74
ResNet-50	24.01	7.02
DenseNet-121	25.02	7.71
CliqueNet	24.98	7.48
SE-ResNet-50	23.29	6.62
SE-CliqueNet	24.01	7.15
CMPE-SE-ResNet-50 (Ours)		
– double FC	23.06	6.46
-1×1 pair-view	22.97	6.41

Table 4: Single crop error rates(%) on ImageNet.

pair-view modes) are slightly better than that of the same level other models, like SE-ResNet-50 (Hu, Shen, and Sun 2018). Compare with SE-ResNet-50, CMPE-SE-ResNet-50 with 1×1 inner-imaging can reduce the top-1 error rate by 0.32%, and the top-5 error rate by 0.21%. The other compared models contain: pre-act ResNet-18, 34, 50 (He et al. 2016b), DenseNet-121 (Huang et al. 2017b), CliqueNet and SE-CliqueNet (Yang et al. 2018), the "SE-CliqueNet" means CliqueNet used channel-wise attentional transition.

Discussion

Compared with the promotion of CMPE-SE module on same level networks, another fact makes us more excited: our CMPE-SE unit can greatly stimulates the potential of smaller networks with fewer parameters, enables them to achieve or even exceed the performance of larger models. This improvement proves that the refined modeling for inner features in convolutional networks is necessary.

About refined modeling of intermediate convolutional features, DenseNet (Huang et al. 2017b) is a type of robust repetitive refining for inner feature maps, in another hand, the "Squeeze and Excitation" (Hu, Shen, and Sun 2018) can also

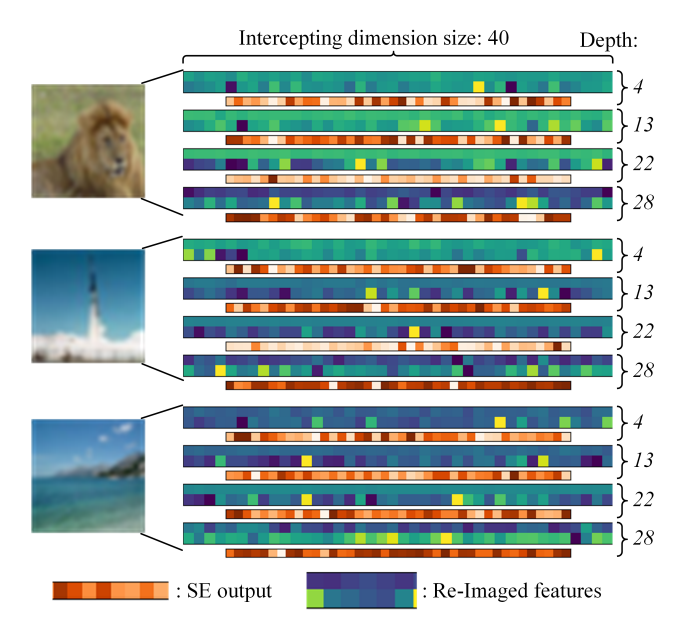


Figure 5: Exsamples of fragmented inner-imaging feature maps and competitive SE outputs from CMPE-SE-WRN-28-10 model with 1×1 pair-view. The green frenulums refer to re-imaged feature maps, the first row comes from identity mapping, the second means residual mapping, the smaller orange frenulums denote the excitation outputs.

be seen as a kind of refined modeling for channel features, and its refining task is learning the relationship of convolution channels. Further, CMPE-SE module extends the task of refined modeling for intermediate features, from the experimental results mentioned above, we can also infer that the intermediate features of ResNet can undertake refined modeling with more tasks.

Actually, in addition to modeling the competitive relationship between residual and identity mappings, the CMPE-SE module also provides the fundamental environment for reimaging the intermediate residual and identity features. To facilitate the display, Fig. 5 shows some examples of fragmented inner-imaging part and the corresponding excitation outputs, these 40 width parts comes from different layers in depth 4, 13, 22 and 28, and we can see that the channel-wise attentional outputs of CMPE-SE block is very vigorous.

In order to reduce the parameter cost generated by the subsequent FC encoder, we average the outputs of pair-view convolution kernels, we also have tried not to do so, then we find that the former can save a lot of parameters and does not sacrifice too much performance. This indicates that the inner-imaging of channel features is parameter-efficient, we can even use a tiny and fixed number of filters to complete pair-view re-imaging.

In the study of this paper, according to the shape of innerimaging feature maps, we have only tried 2×1 and 1×1 two types pair-view filters, which can achieve aforementioned results. So, we have reason to believe that branch competitive modeling and inner-imaging can bring more capacious reimaged feature maps and diverse refined modeling structure, on multi-branch networks.

Conclusion

In this study, we present a competitive squeeze and excitation block for ResNets, which model the competitive relation from both residual and identity channels, and expand the task of channel-wise attentional modeling. Further, we introduce the inner-imaging strategy to explore the channel relationship by convolution, on re-imaged feature maps. The proposed design uses a few extra parameters and can be easily applied on any types of residual network. We evaluate our models on three publicly available datasets against state-of-the-art results, our approach can improve the performance of ResNets and stimulate the potential of smaller networks. Moreover, the presented method is extremely scalable and has potential to play a greater role in multi-branch architectures.

Acknowledgements

This work was supported by a China National Science Foundation under Grants (60973083, 61273363), Science and Technology Planning Projects of Guangdong Province (2014A010103009, 2015A020217002), and Guangzhou Science and Technology Planning Project (201504291154480).

References

[Ahmed and Torresani 2017] Ahmed, K., and Torresani, L. 2017. Connectivity learning in multi-branch networks. *arXiv:1709.09582*.

[Chang et al. 2018] Chang, B.; Meng, L.; Haber, E.; Ruthotto, L.; Begert, D.; and Holtham, E. 2018. Reversible architectures for arbitrarily deep residual neural networks. *AAAI*.

[Chen et al. 2016] Chen, L.; Yang, Y.; Wang, J.; Xu, W.; and Yuille, A. L. 2016. Attention to scale: Scale-aware semantic image segmentation. *CVPR*.

[Chen et al. 2017a] Chen, L.; Zhang, H.; Xiao, J.; Nie, L.; Shao, J.; Liu, W.; and Chua, T. 2017a. Sca-cnn: Spatial and channel-wise attention in convolutional networks for image captioning. *CVPR*.

[Chen et al. 2017b] Chen, Y.; Li, J.; Xiao, H.; Jin, X.; Yan, S.; and Feng, J. 2017b. Dual path networks. *NIPS*.

[Chen et al. 2018] Chen, T. Q.; Rubanova, Y.; Bettencourt, J.; and Duvenaud, D. 2018. Neural ordinary differential equations. *arXiv:1806.07366*.

[Deng et al. 2009] Deng, J.; Dong, W.; Socher, R.; Li, L.; Li, K.; and Feifei, L. 2009. Imagenet: A large-scale hierarchical image database. *CVPR*.

[Figurnov et al. 2017] Figurnov, M.; Collins, M. D.; Zhu, Y.; Zhang, L.; Huang, J.; Vetrov, D. P.; and Salakhutdinov, R. 2017. Spatially adaptive computation time for residual networks. *CVPR*.

[Han, Kim, and Kim 2017] Han, D.; Kim, J.; and Kim, J. 2017. Deep pyramidal residual networks. *CVPR*.

[He et al. 2016a] He, K.; Zhang, X.; Ren, S.; and Sun, J. 2016a. Deep residual learning for image recognition. *CVPR*.

[He et al. 2016b] He, K.; Zhang, X.; Ren, S.; and Sun, J. 2016b. Identity mappings in deep residual networks. *ECCV*.

- [Hu, Shen, and Sun 2018] Hu, J.; Shen, L.; and Sun, G. 2018. Squeeze-and-excitation networks. *CVPR*.
- [Huang et al. 2016] Huang, G.; Sun, Y.; Liu, Z.; Sedra, D.; and Weinberger, K. Q. 2016. Deep networks with stochastic depth. *ECCV*.
- [Huang et al. 2017a] Huang, G.; Chen, D.; Li, T.; Wu, F.; Der Maaten, L. V.; and Weinberger, K. Q. 2017a. Multiscale dense convolutional networks for efficient prediction. *arXiv*: 1703.09844.
- [Huang et al. 2017b] Huang, G.; Liu, Z.; Der Maaten, L. V.; and Weinberger, K. Q. 2017b. Densely connected convolutional networks. *CVPR*.
- [Ioffe and Szegedy 2015] Ioffe, S., and Szegedy, C. 2015. Batch normalization: Accelerating deep network training by reducing internal covariate shift. *ICML*.
- [Jaderberg et al. 2015] Jaderberg, M.; Simonyan, K.; Zisserman, A.; and Kavukcuoglu, K. 2015. Spatial transformer networks. *NIPS*.
- [Krizhevsky, Sutskever, and Hinton 2012] Krizhevsky, A.; Sutskever, I.; and Hinton, G. E. 2012. Imagenet classification with deep convolutional neural networks. *NIPS*.
- [Krizhevsky 2009] Krizhevsky, A. 2009. Learning multiple layers of features from tiny images.
- [Larsson, Maire, and Shakhnarovich 2017] Larsson, G.; Maire, M.; and Shakhnarovich, G. 2017. Fractalnet: Ultra-deep neural networks without residuals. *ICLR*.
- [Li, Zhu, and Gong 2018] Li, W.; Zhu, X.; and Gong, S. 2018. Harmonious attention network for person re-identification. *CVPR*.
- [Linsley et al. 2018] Linsley, D.; Dan, S.; Eberhardt, S.; and Serre, T. 2018. Global-and-local attention networks for visual recognition. *arXiv:1805.08819*.
- [Netzer et al. 2011] Netzer, Y.; Wang, T.; Coates, A.; Bissacco, A.; Wu, B.; and Ng, A. Y. 2011. Reading digits in natural images with unsupervised feature learning. *NIPS. Workshop*.
- [Newell, Yang, and Deng 2016] Newell, A.; Yang, K.; and Deng, J. 2016. Stacked hourglass networks for human pose estimation. *ECCV*.
- [Nguyen, Zhao, and Yan 2018] Nguyen, T. V.; Zhao, Q.; and Yan, S. 2018. Attentive systems: A survey. *International Journal of Computer Vision*.
- [Perez et al. 2018] Perez, E.; Strub, F.; De Vries, H.; Dumoulin, V.; and Courville, A. C. 2018. Film: Visual reasoning with a general conditioning layer. *AAAI*.
- [Real et al. 2018] Real, E.; Aggarwal, A.; Huang, Y.; and Le, Q. V. 2018. Regularized evolution for image classifier architecture search. *arXiv*: 1802.01548.
- [Simonyan and Zisserman 2015] Simonyan, K., and Zisserman, A. 2015. Very deep convolutional networks for large-scale image recognition. *ICLR*.
- [Stollenga et al. 2014] Stollenga, M. F.; Masci, J.; Gomez, F. J.; and Schmidhuber, J. 2014. Deep networks with internal selective attention through feedback connections. *NIPS*.

- [Sun et al. 2018] Sun, M.; Yuan, Y.; Zhou, F.; and Ding, E. 2018. Multi-attention multi-class constraint for fine-grained image recognition. *arXiv*:1806.05372.
- [Szegedy et al. 2015] Szegedy, C.; Liu, W.; Jia, Y.; Sermanet, P.; Reed, S. E.; Anguelov, D.; Erhan, D.; Vanhoucke, V.; and Rabinovich, A. 2015. Going deeper with convolutions. *CVPR*.
- [Szegedy et al. 2016] Szegedy, C.; Vanhoucke, V.; Ioffe, S.; Shlens, J.; and Wojna, Z. 2016. Rethinking the inception architecture for computer vision. *CVPR*.
- [Veit, Wilber, and Belongie 2016] Veit, A.; Wilber, M. J.; and Belongie, S. J. 2016. Residual networks behave like ensembles of relatively shallow networks. *NIPS*.
- [Wang et al. 2017a] Wang, F.; Jiang, M.; Qian, C.; Yang, S.; Li, C.; Zhang, H.; Wang, X.; and Tang, X. 2017a. Residual attention network for image classification. *CVPR*.
- [Wang et al. 2017b] Wang, X.; Yu, F.; Dou, Z.; and Gonzalez, J. E. 2017b. Skipnet: Learning dynamic routing in convolutional networks. *arXiv*: 1711.09485.
- [Wang et al. 2018] Wang, Y.; Xie, L.; Qiao, S.; Zhang, Y.; Zhang, W.; and Yuille, A. L. 2018. Multi-scale spatially-asymmetric recalibration for image classification. *arXiv:* 1804.00787.
- [Wu et al. 2018] Wu, Z.; Nagarajan, T.; Kumar, A.; Rennie, S.; Davis, L. S.; Grauman, K.; and Feris, R. S. 2018. Blockdrop: Dynamic inference paths in residual networks. *CVPR*.
- [Xie and Yuille 2017] Xie, L., and Yuille, A. L. 2017. Genetic cnn. *ICCV*.
- [Xie et al. 2017] Xie, S.; Girshick, R. B.; Dollar, P.; Tu, Z.; and He, K. 2017. Aggregated residual transformations for deep neural networks. *CVPR*.
- [Yang et al. 2018] Yang, Y.; Zhong, Z.; Shen, T.; and Lin, Z. 2018. Convolutional neural networks with alternately updated clique. *CVPR*.
- [Zagoruyko and Komodakis 2016] Zagoruyko, S., and Komodakis, N. 2016. Wide residual networks. *BMVC*.
- [Zhang et al. 2017a] Zhang, T.; Qi, G.; Xiao, B.; and Wang, J. 2017a. Interleaved group convolutions for deep neural networks. ICCV.
- [Zhang et al. 2017b] Zhang, X.; Li, Z.; Loy, C. C.; and Lin, D. 2017b. Polynet: A pursuit of structural diversity in very deep networks. *CVPR*.
- [Zhang et al. 2018a] Zhang, H.; Cisse, M.; Dauphin, Y. N.; and Lopezpaz, D. 2018a. mixup: Beyond empirical risk minimization. *ICLR*.
- [Zhang et al. 2018b] Zhang, X.; Zhou, X.; Lin, M.; and Sun, J. 2018b. Shufflenet: An extremely efficient convolutional neural network for mobile devices. *CVPR*.
- [Zheng et al. 2017] Zheng, H.; Fu, J.; Mei, T.; and Luo, J. 2017. Learning multi-attention convolutional neural network for fine-grained image recognition. *ICCV*.
- [Zoph et al. 2018] Zoph, B.; Vasudevan, V.; Shlens, J.; and Le, Q. V. 2018. Learning transferable architectures for scalable image recognition. *CVPR*.